SOURCE ENERGY SPECTRA FROM DEMODULATION OF SOLAR PARTICLE DATA BY INTERPLANETARY AND CORONAL TRANSPORT

J. Pérez-Peraza*, M. Alvarez-Madrigal*, and F. Rivero*
Instituto de Geofísica, UNAM, 04510- C.U., México 20, D. F., MEXICO

L. I. Miroshnichenko
IZMIRAN, Troitsk, Moscow Region, 142092, USSR

1. Introduction. The data on source energy spectra of solar cosmic rays (SCR), i.e. the data on the spectrum form and on the absolute SCR are of great interest at least for three reasons: 1) the SCR contain the energy comparable to the total energy of electromagnetic flare radiation ($\leq 10^{32}$ ergs); 2) the source spectrum form indicates to a possible acceleration mechanism (or mechanisms); and 3) the accelerated particle are efficiently involved in nuclear electromagnetic and plasma processes in the solar atmosphere. Therefore the data on SCR source spectra are necessary for theoretical description of the processes mentioned and for the formulation of the consistent flare model. Below it is attempted to sound solar particle sources by means of SCR energy spectrum obtained near the Sun, at the level of the roots of interplanetary field lines in the upper solar corona. We consider data from ∿ 60 solar proton events (SPE) between 1956-1981 [1]. These data were obtained mainly by the interplanetary demodulation of observed fluxes near the Earth. Further, we used our model of coronal azimuthal transport to demodulate those spectra, and to obtain the source energy spectra.

2. Interplanetary Demodulation. Several methods are used for the interplanetary demodulation of SCR fluxes observed near the Earth. Most of them are traditionally based on the different modifications of the diffusion model of the full transport equation. In addition, at present the possibility exists to reconstruct the source spectrum by the gamma-ray and flare neutron data. The diffusion methodics of interplanetary demodulation was described in detail in another works [2, 3]. This methodics rest upon the extrapolation of intensity time profiles of SCR fluxes observed near the Earth to the momentum of their injection from the solar corona. Each of modifications of such a methodics is applicable only to a limited time interval or to a limited range of particle energy. Besides that, our Catalogue [1] contains some discrepancies and gaps in spectrum parameter estimations obtained by the different researchers. Because of these reasons we were able to use for the coronal demodulation only the data of 26 events.

3. Coronal Demodulation. The coronal transport model of solar flare particles was discussed in [4] and extensively described in [5]. Basically two transport steps take place in azimuthal coronal transport of particles: (a) a velocity-independent transport in a fast propagation region (FPR) which is associated with an expanding magnetic structure, (b) an energy-dependent transport in a low propagation region (LPR), dominated by transversal diffusion, drifts and gradual escape into the interplanetary space. The initial condition for the 2nd transport state, when particles are globally liberated from the FPR, at t=0 is $N(X,0)=N_a(E)/X_o$, if X is within the width X_o of the FPR centered at the flare site, and $N(X, 0)=0$ elsewhere, where $N_a(E)$ is the flare source energy spectrum. The azimuthal evolution of the number density of particles at time t and position X during the 2nd transport step is [4, 5].

---

*On leave for the INAOE, Tonanzintla, A.P. 51. 72000-Puebla.México

$$N(X,t)=2.5N_a\exp\left(-\Gamma t-\frac{(X-v_dt)^2+(X_\circ/2)}{8\kappa_\ell t}\right)\left\{\exp\left[\frac{(X-v_dt)(X_\circ/2)}{4\kappa_\ell t}+\frac{(X-v_dt-X_\circ/2)^2}{8\kappa_\ell t}\right]\mathrm{erf}\left(\frac{X-v_dt-X_\circ 2}{(4\kappa_\ell t)^{0.5}}\right)-\exp\left[-\frac{(X-v_dt)(X_\circ/2)}{4\kappa_\ell t}+\frac{(X-v_dt+X_\circ/2)^2}{8\kappa_\ell t}\right]\mathrm{erf}\left(\frac{X-v_dt+X_\circ/2}{(4\kappa_\ell t)^{0.5}}\right)\right\} \quad (1)$$

where κ_ℓ and v_d are the transversal diffusion coefficient and drift velocity. Here after we will refer our results to the flare position (X_f), such that $X_i=X-X_f$. For coronal demodulation we adopted the following procedure. We assume that the observed particle flux proceeds from a coronal longitude at ∿ 60°W; so, at the coronal level the observed flux corresponds at the position $X_c=X(60°W)-X_f$, and an ejection time from the corona (t_e) given as $t_e=0$ if $|X_c|\leq X_\circ/2$ and $t_e=|X_c|/v_d$ if $|X_c|>X_\circ/2$; next we equate (2) with the demodulated energy spectra N(E) from [3], [that for the task of simplicity we translated from rigidity to kinetic energy, Figs.(1) and (2)]:

$$2.5N_a(E)f[X_c,t_e,v_d(E),\kappa_\ell(E),X_\circ] = N(E)\ (\mathrm{part/MeV}) \quad (2)$$

so that the source energy spectrum $N_a(E)=N(E)/2.5f[X_c,t_e,v_a,\kappa_\ell,X_\circ]$, where the function f has been normalized. Once we have determined $N_a(E)$ (part/MeV) we build the time-profiles by fixing the positions X_i and energy E_i in eq.(1), and making vary time relative to t_{on}, $(t-t_{on})$, where $t_{on}=(|X_i|/v_d)-X_\circ/2$ is the onset time of particle arrival at that particular position X_i, so that the time-origin occurs at $t=t_{on}$. The coronal time-profiles were built for several coronal positions and energy values. To build the particle azimuthal distributions we fixed energy and time in eq.(1) and evaluated for $X_i\leq\pm180°$ taking the flare position as the coordinate-origin. Further, we evaluated for other times and different energies. For calculations we assumed for the FPR, an azimuthal width at its opening of 80° at 0.9 $R_\odot$ above the photosphere. For $v_d=(60\text{-}250)\beta^2/(1-\beta^2)^{0.5}$(cm/s) depending on whether the observational peak intensity was very late or early respectively, where $\beta=v/c$, v and c are the particle and light velocities. We used $\kappa_\ell=6.7\times10^6v$(cm^2/s). For the task of illustration we have chosen an event which FPR contains the connecting position X_c(23/VI/1956) and other which FPR does not contain X_c(22/VIII/1958). On the next figures we have illustrated linear azimuthal positions X_i in terms of angular coordinates Ψ_i; on Fig.(2) we show along with the demodulated spectrum the energy spectra that we have built for two others coronal longitudes. On figures (3)-(8) it is shown the azimuthal distributions of both events for several times at three different energies. It can be observed that the observational W-E asymmetry is confirmed by our results: the higher the particle energy the sharped the effect. Theoretically this is the translation of particle drift in the model. On figs. (9)-(11) it is show the time profiles of the event for which X_c is outside of its FPR, for 3 different energies and several longitudinal positions· out of the FPR profiles show the characteristic diffusive shape, whereas at locations within the FPR they show a peculiar decreasing shape. On Fig. (12) it is shown the regression in time from the corona back to the top of the FPR: since regression in time is equivalent to regression in distance to the FPR, for a given value of Ψ any other Ψ' such that $\Psi_f<\Psi'<\Psi$ can be seen as a time regression toward the time of particle liberation from the FPR. In fact time profiles at $\Psi_f \pm 40°$ begin at t=0. Out of the FPR the onset is delayed proportionally to the distance from the flare site, such as indicated by observations. Fig.(13) shows the west-asymmetry effectrelative to the profile on Fig. (9): at 50°-distance from the flare on the East side there is more of 10^2 time less particles than at the same distance an the West side, and at 60°-distance the flux has fallen to negligeable levels relative to the West side. On figs. (14)-(16) we show time profiles for the 23/11/1956 event. Concerning source energy spectra, it is obvious that according to the coronal transport model the observational and the source spectra are basically the same when the FPR contains the connection longitud. So, among the studied 26 events, only in 8 events the FPR does not contain X_c. We have tabulated on Table 1, the source spectra characteristics of these 8 events along with one (23/11/1956) of the remaining 18 events where N_a=N(E). On Fig.(17) we show the source spectrum $N_a = D_o E^{-\gamma} = 4.18 \times 10^{45} E^{-6.36}$ (part./MeV) of the 22/VIII/1958 event. Finally, on Fig. (18) it is illustrated the source spectrum $N_a/\delta\Psi_f$ (part./MeV cm) under the assumption of a finite flare width $\delta\Psi_f = 8°$ and the spectrum at the top of the FPR at t=0, N(X,t,E)= N_a/X_o(part./MeV cm).

4. Conclusions. Though results are model-dependents they furnish a clear picture of the evolution of particle energy spectra from the source till their ejection into the interplanetary space, for those events where the observational-connecting-longitude is out of the FPR: it can be seen in Table 1 that energy spectra flattens at the coronal level relative to the source spectra; when particles move in the W-E direction, as in the 1/IX/1971 event, the change in spectrun slope is more important. It is interesting to analyze our results within the frame of the observational effects and model predictions sumarized in [5]. We believe that this approach must be taken into account within the frame of solar particle acceleration theory and solar flare phenomena, such as for the evaluation of flare neutrons and electromagnetic radiation of non-thermal origin.

References

[1] Miroshnichenko, L.I.,Preprint IZMIRAN,15,548, 1985.
[2] Miroshnichenko, L. I., Geomagn. and Aeron. 13, 26, 1973.
[3] Miroshnichenko, L. I. et al.,Dynamics of Radiation Conditions in Space, Energoatmizdat, Moscow, 1985(with Petrov V M.)
[4] Pérez-Peraza,J.and Martinell,J.,Proc. 17th Int.Cosmic Ray Conf.3. 55,1981.
[5] and Pérez-Peraza J. in Invited Lecture,9th European Cosmic Ray Simposium,Kosice,1985.

		CORONAL			SOURCE Na	
EVENT	LONGI-TUDE	RANGE MeV	Dc PART/MeV	γ_E	Do PART/MeV	γ_E
23/02/1956	23N80W	35 - 480	2.10E37	1.27	2.1E37	1.27
22/08/1958	18N10W	15 - 115	5.77E39	3.74	4.1E45	6.36
03/09/1960	18N89E	10 - 410	2.91E36	2.02	1.4E53	8.76
28/09/1961	13N29E	15 - 470	1.97E39	3.20	4.6E53	8.76
28/01/1967	150E	75 - 410	5.16E34	1.25	1.1E40	3.11
29/09/1968	13N13W	10 - 160	1.01E34	1.48	2.9E43	5.76
01/09/1971	12S130W	10 - 55	1.43E39	2.25	4.9E45	6.33
28/05/1972	09N30E	30 - 75	1.22E37	2 62	4.1E40	4.14
--'--'----	-'--'-	30 - 120	1.00E34	2.20	2.6E38	4.03

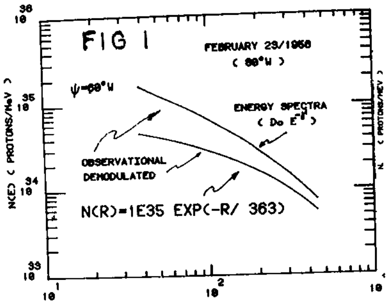
FIG 1

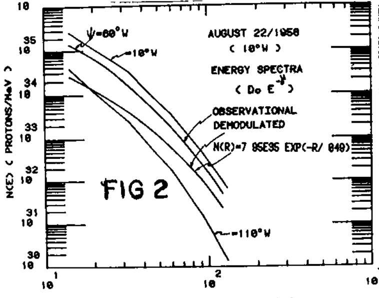
FIG 2

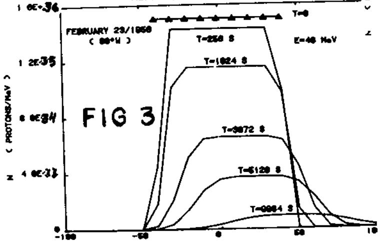
FIG 3

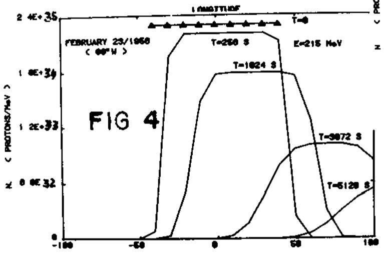
FIG 4

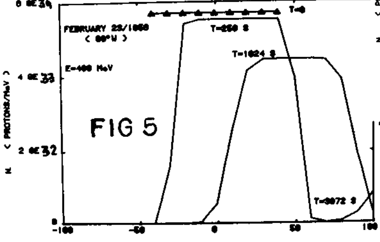
FIG 5

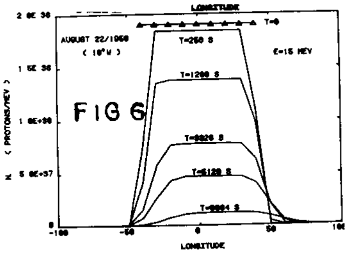
FIG 6

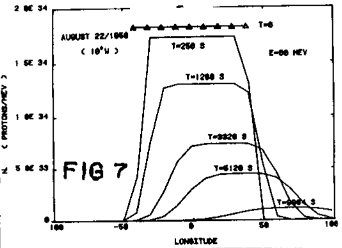
FIG 7

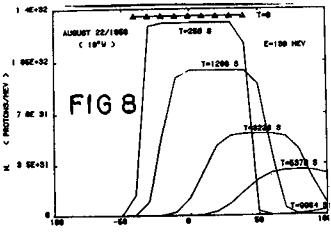
FIG 8

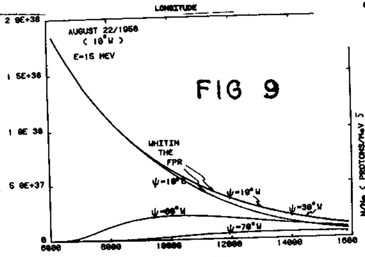
FIG 9

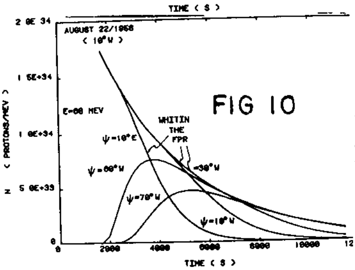
FIG 10

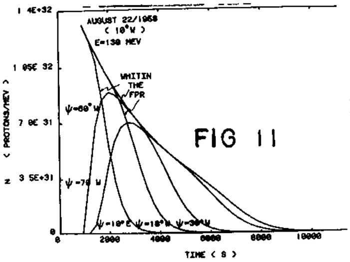
FIG 11

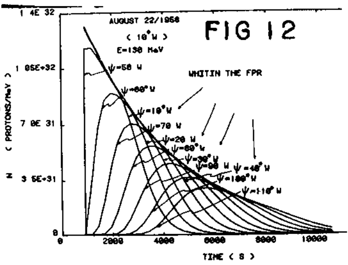
FIG 12

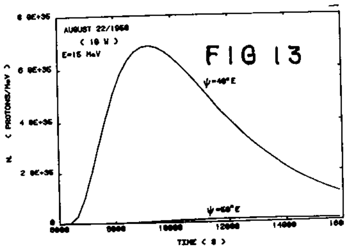
FIG 13

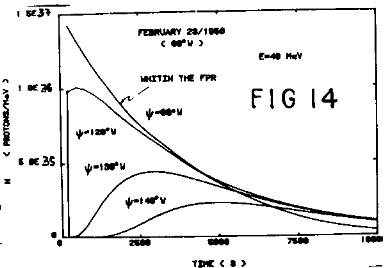
FIG 14

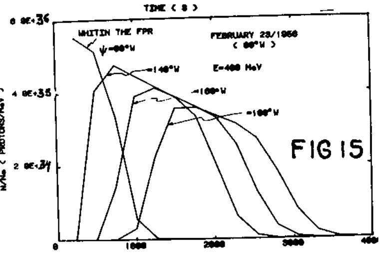
FIG 15

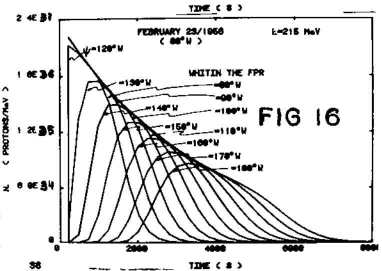
FIG 16

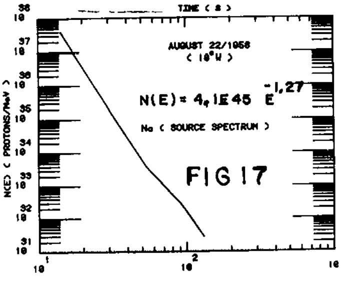
FIG 17

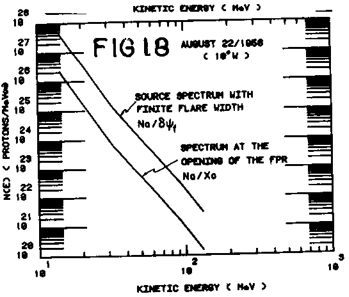
FIG 18